Interfacial strain-induced self-organization in semiconductor dielectric gate stacks. I. Strain relief at the $Si-SiO_2$ interface

G. Lucovsky[a)]
Department of Physics, North Carolina State University, Raleigh, North Carolina 27695-8202

J. C. Phillips
Department of Physics, Rutgers University,Piscataway, New Jersey 08854

(Received 18 January 2004; accepted 26 April 2004; published 19 August 2004)

It has been demonstrated that $Si-SiO_2$ interfaces in field effect transistors are not atomically abrupt, but instead contain: (i) an interfacial transition region ~0.5 nm thick with an average SiO composition as well as (ii) a strained or defective region in the Si substrate that is of similar extent. The strain profile across these interfacial transition regions, compressive in the SiO_2 and tensile in the Si substrate, results from a combination of growth induced strain, as well as differences between the linear expansion coefficients of SiO_2 and the substrate Si. Two high-temperature transitions modify the strain profile, and the transition region bonding at the $Si-SiO_2$ interface. The first is a visco-elastic relaxation in the SiO_2 occurring at ~1000 °C, and the second is associated with bonding changes within the interfacial transition region occurring at ~900 °C. This article uses spectroscopic studies to identify the chemical bonding changes within the interfacial transitions region that occur after 900 °C annealing in an inert ambient. The physical and chemical forces that drive these changes are addressed from two perspectives: (i) reactions kinetics and (ii) bond constraint theory. Finally the effects of strain relief on device performance and reliability are discussed. © *2004 American Vacuum Society.* [DOI: 10.1116/1.1771676]

I. INTRODUCTION

Several experimental studies have demonstrated that the interface between Si and SiO_2 in field effect transistor (FET) devices which have been subjected to conventional high temperature processing are not atomically abrupt, but instead contain an interfacial transition region with Si sub-oxide, SiO_x, $x<2$, bonding.[1–3] This article briefly reviews these studies, and develops a strain profile for $Si-SiO_2$ gate stacks that includes a significant strain gradient across the interfacial transition region. The article focuses on experimental studies that have explored changes in bulk stain and interfacial bonding as a function of postoxidation annealing in inert ambients.[4–6] These studies have distinguished between two different transitions: (i) one at ~1000 °C in which growth is induced in the SiO_2 layer and (ii) a second at ~900 °C in which there are changes in the bonding within the interfacial transition region between the Si substrate and the SiO_2. This article identifies the microscopic physical and chemical forces that drive the $Si-SiO_2$ interfacial transition region bonding rearrangements during the 900 °C anneal.

Interfacial properties play a significant role in determining device performance as well as device reliability. The insights gained from the approach of this paper are important in aggressively scaled FET devices in which the physical thickness of the SiO_2 gate dielectric has been reduced in the nanometer regime, <3 nm and extending to between at least 1.4 and 1.5 nm, This approach is also important for future generations of FET devices that extend scaling into a regime in which tunneling leakage through SiO_2 is too high for device operation, and in which alternative high-*k* dielectrics provide a pathway to increasing the gate dielectric capacitance, while maintaining tunneling leakage currents at levels consistent with performance and reliability targets for more aggressively scaled devices.[7,8] These scaled devices require that the equivalent oxide thickness (EOT) be reduced below 1.0 nm.[7,8] EOT is defined as the SiO_2 thickness corresponding to the entire gate stack, including the high-*k* alternative dielectric, as well as an interfacial SiO_2 layer. Since the lower dielectric constant of this interfacial layer places a significant limitation of the smallest attainable values of EOT, it is important to understand the role the interfacial transition regions play in meeting scaling targets for advanced devices addressed in the International Technology Roadmap for Semiconductors.[8]

II. BACKGROUND

Several studies have established that the SiO_2 interface was neither abrupt on atomic scaling of bonding, nor strain free.[1–3] In addition, have identified two different temperature dependent strain relaxations that will be explained by the extension of bond constraint theory (BCT), as originally proposed to explain glass formation in network solids such as As_2S_3 and SiO_2,[9,10] to semiconductor dielectric interfaces, and internal dielectric interfaces as well.[11]

Three factors contribute to the formation of the Si suboxide interfacial transition regions at $Si-SiO_2$ interfaces. Differences in the Si–Si interatomic distances in the crystalline Si substrate, 0.235 nm, and the SiO_2 dielectric, ~0.305 nm, generate intrinsic growth compressive stress in the oxide and tensile stress in the substrate. These differences in inter-

a)Electronic mail: lucovsky@unity.ncsu.edu

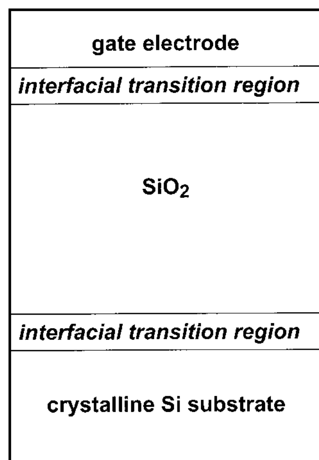

FIG. 1. Schematic representation of interface bonding, including a strained Si substrate layer Si_D, an interfacial transition region with an average SiO composition, an SiO_2 dielectric, a second interfacial region, and a gate metal.

atomic distances have also been cast in terms of a molar volume mismatch between Si and the SiO_2 that is created by a thermal oxidation or plasma deposition process.[12] Differences in linear thermal expansion coefficients in the SiO_2 dielectric ($\sim 0.5 \times 10^{-6}\,C^{-1}$) and the Si substrate ($\sim 2.5 \times 10^{-6}\,C^{-1}$) contribute an additive thermally induced strain component that is equivalent to a bond strain approaching several tenths of a percent for oxides grown or processed at 800–1000 °C and then cooled down to room temperature. Finally, and providing the connection with BCT, there are significant differences in the average number of bonds per atom N_{av} in the Si substrate (4) and the SiO_2 bulk film (2.67), which contribute to bond strain on the atomic scale.

A. Local bonding arrangements at the Si–SiO_2 interface

Studies by medium ion energy scattering on Si(111)–SiO_2 interfaces identified interfacial transition regions with suboxide bonding, and defective Si interfacial regions, defined as Si_D (see Fig. 1).[1] The scattering was studied as a function of the SiO_2 layer thickness, and compared with models that included a strained or defective layer within the Si substrate Si_D. The best fit to the observed scattering was obtained with a two–three atom thick reconstructed substrate Si approximately 0.5 nm thick, and a Si suboxide interfacial transition layer with an average composition of SiO, and an approximate thickness of 0.35 ± 0.1 nm.

Spectroscopic ellipsometry (SE) studies confirmed the SiO_x interfacial transition regions, but did not include a defective Si substrate layer in the model for analysis of the complex dielectric constants.[2] Spectroscopic dielectric functions obtained from analysis of the experimental data were compared with a model that included previously tabulated dielectric constants for bulk Si and bulk SiO_2 as well as a void fraction at the top of the SiO_2 film to emulate surface roughness. The best fit to the data was obtained by including a 0.75 ± 0.2 nm interfacial transition region with an average composition of SiO to the modeled interface structure. It is our opinion that inclusion of a defective Si_D layer in the analysis would have reduced the thickness of the SiO layer, and brought the SE results in closer agreement with the ion scattering studies.[1]

Interfacial suboxide layers have also been studied by synchrotron, or soft x-ray photoelectron spectroscopy (SXPS).[3,6] Using monochromatic soft x-ray radiation ~150–200 eV from a synchrotron gives enhanced surface sensitivity. By adjusting the final kinetic energy of the photoemitted electrons to an energy of ~50–100 eV corresponding to an ~0.6 nm escape depth, Himpsel and his collaborators[3] identified four Si pp core level spectral features that were chemically shifted with respect to the substrate peak Si. These studies had sufficient resolution to spectroscopically resolve the $2p_{1/2}$ and $2p_{3/2}$ spin–orbit split components, making it relatively easy to identify the energy separations between these four core level components. In order of increasing core level binding energy, these features were assigned to three suboxide bonding features associated with Si bonded to one Si^{1+}, two Si^{2+}, and three Si^{3+}, O atoms, and a bulk SiO_2 feature, Si^{4+}, in which each Si atom had four O atom nearest neighbors. In the same notation the Si substrate peak has been denoted as Si^0. Although there has been some controversy relative to these assignments, based primarily on different models for core-level chemical shifts, the initial assignments of Himpsel and co-workers[3] have stood the test of time, and have been applied in the temperature dependent studies discussed in this article.[6]

B. Relaxation of growth strain in Si–O_2 gate stacks

Single wavelength ellipsometry studies using a 632.8 nm He–Ne laser were performed on thermally grown SiO_2 on Si(111) faces, and subjected to furnace annealing in flowing Ar.[12] The SiO_2 films were grown by conventional thermal oxidation in dry O_2 at 850 °C to a nominal thickness of 125 nm and were then furnace annealed in Ar for 30 min at temperatures up to 1100 °C. The data indicated: (i) decreases in the optical index of refraction n at 632.8 nm, with a threshold of about 950 °C and a maximum rate of change at approximately 1050 °C and (ii) a complementary increase in film thickness also with a threshold at about 950 °C and a maximum rate of change at approximately 1050 °C. These changes have been attributed in Ref. 12 to relaxation of intrinsic growth stress. As the stress is relieved in the growth direction, the film thickness increases, and the density of the SiO_2 decreases leading to reductions in the index of refraction that track linearly with the increased physical thickness. After the high temperature anneals and cool down, there is a residual component of compressive stress in the SiO_2, and tensile stress in the Si substrate that results from the differences between the respective Si and SiO_2 linear coefficients of thermal expansion.

The combination of optical second harmonic generation (SHG),[4] and the single wavelength ellipsometry measurements discussed above has identified a second transition at a temperature of approximately 900 °C. This transition has

been attributed to bonding changes at the Si–SiO_2. Contributions to an optical second harmonic response from a surface, bulk, or interface, as for example the generation of coherent light at a photon energy of 2ω when the medium is exposed to intense illumination at a photon energy of ω from a high power laser.[4,13] Applied to Si–SiO_2 interfaces, no SHG signal is expected from either: (i) the noncrystalline SiO_2 layer, due to lack of long range order required for development of a coherent electric field component at 2ω or (ii) the crystalline Si substrate because of the local symmetry at the Si atom bonding sites. In contrast, SHG, is possible Si surfaces and Si–SiO_2 interfaces, with matrix elements, including resonance energies, being different for different interface bonding arrangements.[13]

An interfacial relaxation had been identified through an analysis of the SHG from response from a vicinal Si(111)–SiO_2 interface, where the vicinal offcut is either in the $11\bar{2}$, or $\bar{1}\bar{1}2$ direction. This was done by studying the azimuthal anisotropy of the SHG signal.[4,13–15] The azimuthal anisotropy is defined with respect to the angle Ψ, between the electrical field and the vicinal off-cut direction for the *pp* polarization in which the *E* fields at ω and 2ω are each perpendicular to the plane of incidence. It is given by

$$E(2\omega)=A_1\cos(\Psi)+A_3\cos(3\Psi)\exp(i\theta), \tag{1}$$

where A_1 and A_3 are the amplitudes of the Fourier components with Ψ and 3Ψ symmetry, respectively. These components are associated with Si–O bonds on terraces, and step edges of offcut surface, and θ is the relative phase angle between these components. The phase angle θ reflects *differences* in a resonance energy associated with the O atom terminated Si bonds on the terraces and at the step edges.[14,15] The off-cut angles in Refs. 4, 14, and 15 ranged from 1° to 5°. Since θ is proportional to sin θ in this angular regime, the ratio A_1/A_3 is proportional to the vicinal off-cut angle.[14,15]

The plot in Fig. 2 gives θ as a function of annealing temperature for a sample prepared by thermal oxidation at ~850 °C, and then annealed to 1050 °C. The largest change in θ is between 850 and 900 °C. This has been interpreted as being due to different bonding relaxations, or rearrangements on the terrace and step edges of the vicinal wafers.[4,14,15] There are smaller changes in θ, between 900 and 1050 °C, and these are assigned to the visco-elastic relaxation of bulk stress discussed above. Interfaces prepared by remote plasma-assisted oxidation at 300 °C gives the same values of θ, to ±2° as the 850 °C thermal oxidation, and additionally the same value of θ, to ±2° after a 900 °C anneal.

III. CHEMICAL BONDING CHANGES ASSOCIATED WITH INTERFACIAL SELF-ORGANIZATION

SXPS[6] and cathodoluminescence spectroscopy (CLS)[5] have provided direct evidence for interfacial bonding changes that occur after a 900 °C anneal. The SXPS studies probe bonding changes at an areal density of 10^{14}–10^{15} cm^{-2}, corresponding to the number of surface bonds per Si atom, while the CLS studies probe these changes at an areal density of ~10^{11}–10^{12} cm^{-2}, corresponding to the scale of interfacial bonding defects.

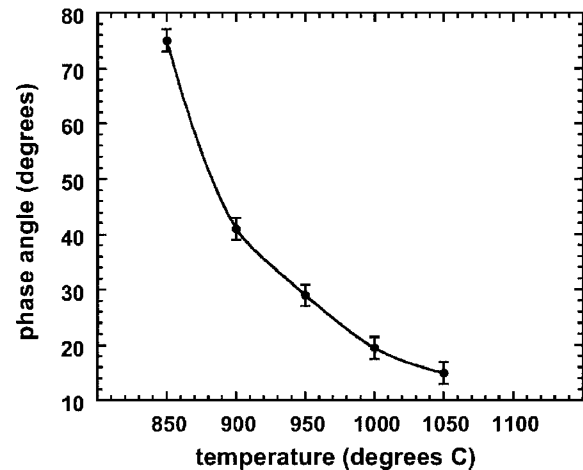

FIG. 2. Phase angle difference between terrace and step edge contributions to the optical SHG signal from vicinal Si(111) wafers off cut 5° in the 112 bar direction. The point at 1100 °C does not fall on the trend line and occurs at temperature at which interface decomposition associated with the evolution of gaseous SiO is known to occur. The solid line is an interpolation that establishes the trend in the data points.

A. SXPS studies

Figure 3 summarizes the results of experiments performed on Si(111) interfaces presented in Ref. 6. The spectral features identified as I_1, I_2, and I_3, correspond, respectively, to bonding arrangements in which Si has one, two and three oxygen neighbors, designated above as Si^{1+}, Si^{2+}, and Si^{3+}. The figure also shows the Si substrate feature Si^0 and

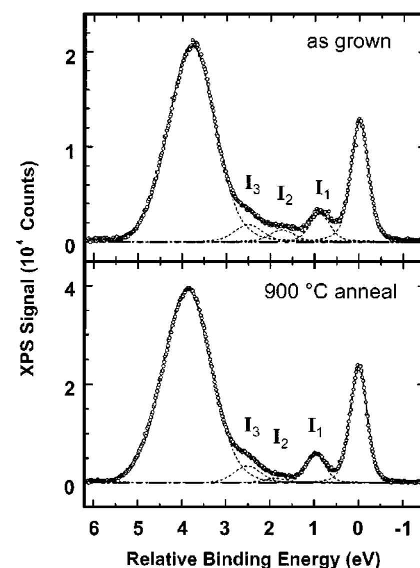

FIG. 3. Spin–orbit stripped and background subtracted Si(2*p*) data for Si(111). (a) shows "as-grown" sample (~1.2 nm) and (b) is for a piece of the same wafer, annealed *ex situ* to 900 °C in Ar. The energy scale is referenced to the substrate Si feature (with four Si neighbors) at 0.0 eV, and the three features marked I_1, I_2, and I_3, are features assigned to Si with one, two, and three oxygen neighbors. The broad feature centered at approximately 4 eV is the SiO_2 features (with four O neighbors) (Ref. 6).

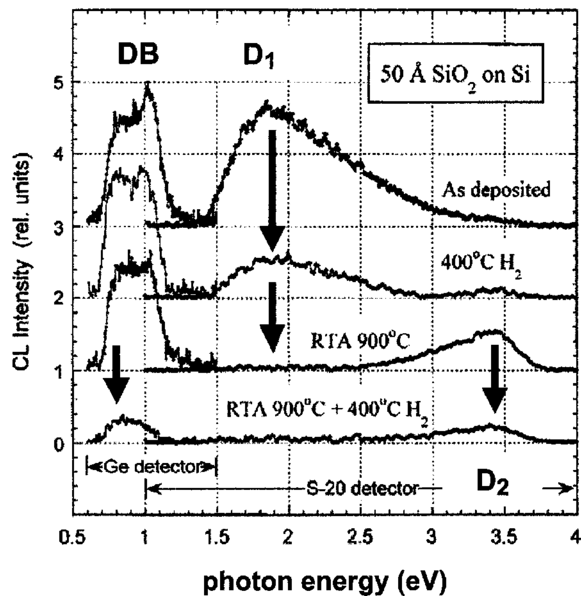

FIG. 4. Process-dependent localized states as revealed by features in the cathodoluminescence spectra in a thin (5 nm) Si–SiO_2 structure. The combination of a RTA and 400 °C anneal under a hydrogen ambient reduces interfacial trap emissions almost completely. The energy of the electron beam (2 keV) has been adjusted to give high sensitivity to luminescence features emanating from the Si–SiO_2 interface region (Ref. 5). The defect luminescence bands are indicated by arrows. DB is an interfacial dangling bond, D_1 is a near interfacial defect in the as-grown transition region prior to the 900 °C RTA, and D_2 is a substrate luminescence band.

the SiO_2 feature Si^{4+}. The samples for this study were prepared by remote plasma processing at 300 °C, and then subjected to annealing at temperatures of 600, 800, 900, and 1000 °C.

The most significant change in the spectra after the 900 °C anneal is a marked reduction in the Si^{2+} component. This is the feature that is *foreign* to a Si(111) interface. Analysis of these spectral changes indicates that after the 900 °C anneal there is 1 monolayer of excess suboxide with an average composition of SiO in excess of a monolayer of Si^{1+} bonding of an abrupt S(111)–SiO_2 interface. As discussed in Ref. 16, this corresponds to a physical thickness of ~0.3–0.4 nm, in good agreement with the ion scattering measurements discussed above. Similar results have been obtained for Si(100)–SiO_2 interfaces, with comparable changes between the as-grown and 900 °C annealed distributions of interfacial bonding arrangements.[6] In the as-grown or as-deposited Si(111) interfaces, the bonding in this SiO transition layer is approximately random with respect to the distribution of the Si^{1+}, Si^{2+}, and Si^{3+} features with a ratio close to 1:2:1. After the 900 °C anneals, it is no longer random, and consists primarily of Si^{1+} and Si^{3+} groups in a ratio of approximately 1:1.

B. CLS studies

These results in Fig. 4 are for an Si–SiO_2 gate stack structure prepared at 300 °C, with a thickness of 5 nm.[5] The CLS spectra were obtained as a function of the electron beam energy, between about 0.5 and 4.5 keV. The spectra in Fig. 4 are for an electron beam energy of 2 keV, and reveal interface and near interface features. Spectra are shown for the as-deposited sample, in which the interface remote plasma-assisted oxidation (~0.6 nm) and SiO_2 remote plasma-enhanced chemical vapor deposition were performed at 300 °C. Additional spectra are shown after a 400 °C hydrogenation anneal in forming gas, 10% H_2/90% N_2, after a 900 °C rapid thermal anneal (RTA) for approximately 1 min in Ar, and after a 900 °C RTA followed by a 400 °C anneal in forming gas. The forming gas anneals terminates Si and O atom dangling bond (DB) defects with a single unpaired electron by creation of a H atom terminated groups, such as Si–H, SiO–H, etc.

As shown in Fig. 4, the combination of a RTA at 900 and 400 °C anneal under a hydrogen ambient significantly reduces interfacial trap cathodoluminescence features. The defect luminescence bands are indicated by arrows. DB, centered at about 1.9 eV, is an interfacial Si atom dangling bond D_1, with a spectral peak at ~1.8 eV is a near interfacial defect, and D_2, with a spectral peak at ~3.4 eV is a substrate luminescence band. The spectral peak and symmetric line shape of the D_1 feature are essentially the same as a photoluminescence (PL) feature reported in Ref. 19 for a Si suboxide with $x \sim 1.1$. The most significant change after the 900 °C RTA and 400 °C H_2 anneal is the reduction of D_1 below the detection limit. The DB defect shows approximately the same reductions as the substrate Si atom dangling bond after a 400 °C H_2 anneal. Comparisons with electrons spin resonance studies of Si(111) interface DBs[17] establish that the DB luminescence as detected by CLS is due to defect bonding changes at the $10^{12}\,cm^{-2}$ level.

IV. BOND STRAIN, THE DRIVING FORCE FOR INTERFACIAL BONDING CHANGES

A study of the stability of homogeneous bulk Si suboxide films deposited at 300 °C, with compositions close to SiO, e.g., SiO_x, $x \sim 1$,[18] demonstrated a chemical phase separation in these films into crystalline Si (c-Si) and noncrystalline SiO_2 (nc-SiO_2) after isochronal annealing in the temperature range from 500 to 1000 °C. This is represented symbolically in Eq. (2) by the following reaction:

$$SiO_x \rightarrow c\text{-Si} + \text{nc-}SiO_2, \quad x \sim 1. \tag{2}$$

This reaction is qualitatively similar to the interfacial transition region chemical bonding changes that have been identified by SXPS.[6] In particular the reaction in Eq. (2) goes to completion in the same temperature range, 850–900 °C, as the interfacial bonding changes of Ref. 6.

PL was detected in the as-deposited homogeneous suboxide samples. PL decreased significantly for increasing annealing temperatures between 650 and 750 °C, and was not detected after the 900 °C anneal. Similar, composition dependent PL features have been reported in other studies, and have been attributed to recombination through intrinsic defect states.[19]

High resolution transmission electron microscopy imaging, coupled with Fourier transformation infrared spectros-

copy (FTIR), confirmed that the as-deposited, homogeneous SiO_x, $x\sim1$ bulk films had chemically phase separated according to Eq. (2). The kinetics of this bulk transition were studied by FTIR to determine the *extent of reaction* as a function annealing temperature. These studies showed the phase separation reaction of Eq. (2) was more than 90% complete after a 900 °C anneal.[18]

The results discussed above have been interpreted in terms of a model that is based on a kinetically limited reaction. This means that the separated material has a lower energy than the homogeneous alloy, but that there is a reaction barrier that must be overcome to separate the homogenous suboxides into the c-Si and nc-SiO_2 reaction products of Eq. (2).

The kinetic limitation is consistent with the equilibrium phase diagram along the tie line between Si and SiO_2, and therefore applies to thin films with a SiO composition that are prepared at low temperature.[18] Below a temperature of 1000 °C, there is no compound phase in along the Si–SiO_2 tie line to trap or hinder the phase separation reaction of Eq. (2).[20] Therefore if the separated products are more stable than the homogeneous suboxide, the separation will be limited by kinetics. The studies discussed in Secs. II and III have demonstrated that changes in bonding in the 1 monolayer thick interfacial transition region between the c-Si substrate and the nc-SiO_2 bulk dielectric occur in approximately the same temperature regime, between about 850 and 900 °C. This comparison suggests that the interfacial chemical reorganization is also limited by reaction kinetics.

The results of Keister *et al.*,[6] indicated that a monolayer scale SiO layer in as-grown oxides, displays random local bonding arrangements, and is converted to Si-rich and O-rich bonding arrangements after a 900 °C anneal. There is insufficient SXPS or SHG data to determine if the temperature dependence of the extent of completion of this interfacial reaction follows the same *trajectory* as the bulk reaction. However, the application of bond constraint theory (BCT) to these two quantitatively different systems suggests that the underlying driving force for the bulk and interfacial chemical phase separations is indeed the same, and involves a reduction of bond-strain energy.

V. BOND CONSTRAINT THEORY

BCT provides a framework for understanding the buildup of strain in network amorphous solids.[11] In network solids in which the constituent atoms are in two-, three-, or fourfold nonplanar bonding arrangements, BCT yields linear relationship between the average number of bonds/atom N_{av} and the total number of valence bond-stretching and bending constraints per atom C_{av} that is given by[9,10]

$$C_{av}=2.5N_{av}-3. \quad (3)$$

BCT provides a remarkably accurate description of network stress in nonideal continuous random network amorphous solids in which $C_{av}>3$, including its consequences with respect to defect formation.[11,21,22] In this article, BTC is extended to the chemical phase separation in SiO_x alloys. These applications of BCT are based on the simple idea that the bonding forces in a network amorphous solid can be arranged in a hierarchy from stronger-stretching to weaker-bending valence forces. The constraining effects of these forces have been shown to be a linear function of the average coordination number N_{av} in Eq. (3). For overconstrained networks such as Si_3N_4 for which $N_{av}=3.43$, and SiO_x with $x\sim1$, for which $N_{av}\sim3$, the Si atom, and N or O atom bond-stretching constraints are stronger than the respective Si atom, and N or O atom bond-bending constraints, so that strain energy accumulates along these bending constraints. The most significant accumulation of strain is at the atomic sites with the lower coordination number N in Si_3N_4 and O in SiO. This means that the average Si–N–Si and Si–O–Si bond angles θ are distorted from their average local values of 120°, and ~150°,[23] by an amount $\delta\theta$, which is proportional to the difference between N_{av} in the nonideal strained network and N^*_{av} in an ideal strain-free network, which has a value of 2.4 so that

$$\delta\theta\propto[N_{av}-N^*_{av}]. \quad (4)$$

Due to an unusually weak bond bending force at the O atoms sites, in SiO_2 one bond-bending constraint is broken, and the effective value of N_{av} is 2.4, rather than 2.67.

It is further assumed that the defect density in overconstrained network solids is associated with broken bonds that relieve the buildup of local strain. As such the density of such defects is expected to be proportional to the strain energy,[20] which is proportional to $[\delta\theta]^2$. Thus, the density of defects D in a constrained network is expected to obey the following scaling relationship:

$$D\propto[N_{av}-N^*_{av}]^2. \quad (5)$$

Intrinsic defects formed in this way are further assumed to be the nucleating centers for the chemical phase separation in SiO_x bulk films. The kinetics of the SiO_x decomposition are then correlated with the defect density in Eq. (5). This mechanism is supported by a decrease in the total strain energy between the as-deposited homogeneous SiO phase, and the chemically separated inhomogeneous diphasic material c-Si+nc-SiO_2.

There are two contributions to strain in the chemically separated SiO_2/c-Si system: (i) the relatively small strain energy in the SiO_2 phase due mostly to (a) the molar volume mismatch as the c-Si/SiO_2 interface, and (b) the difference in thermal expansion coefficients between c-Si and nc-SiO_2 and (ii) an interfacial strain energy. There is no strain in the c-Si component, except for a small amount tensile strain at the interface. This is contrasted with the relatively high levels of strain in the SiO homogenous films, in which C_{av} is increased from ~3 in SiO_2 to 4.2. This argument for a reduced strain energy in the phase-separated alloy is supported by the experiments reported in Ref. 18, which demonstrated that the chemically phase separated systems showed no detectable luminescence, indicative of a low density of interfacial defects at the interfaces between the c-Si and SiO_2 constituents of the diphasic material.

The discussion presented above suggests that the changes in bonding at the $Si–SiO_2$ interface after a 900 °C anneal in an inert ambient are also driven by a strain relief mechanism. In this model, interfacial defects in the as-grown interfacial transition region are the nucleating centers for the chemical separation of that region into Si-rich and O-rich domains. This is consistent with a nanoscale separation that is correlated with the density of Si dangling bonds in the substrate, $\sim 5\times 10^{12}\,cm^{-2}$.[17] If these dangling bond defects are the nucleating centers, then the characteristic dimension r for interfacial chemical reorganization is estimated by setting

$$r \approx d(\mathrm{Si-Si})_{\mathrm{Si}(100)}\left(\frac{1}{\sqrt{f_{\mathrm{db}}}}\right), \qquad (6)$$

where f_{db} is the fraction of dangling bonds, and $d(\mathrm{Si-Si})_{\mathrm{Si}(100)}$ is the interatomic spacing between Si atoms on the Si(100) surface. This gives a characteristic scaling parameter of approximately 5 nm.

VI. BCT MODEL FOR INTERFACIAL SELF-ORGANIZATION

Lucovsky and Phillips and co-workers applied the concepts of constraint theory developed to explain glass formation in chalcogenide and oxide glasses,[11,12] to Si–dielectric interfaces[21,22] in which there was a discontinuity in N_{av}, and therefore also C_{av} at a dielectric interface. This approach has provided important insights to the physical mechanisms underlying: (i) the formation of interfacial transition regions and (ii) defect formation and defect relaxation at these interfaces.[24] The approach builds on the studies of Boolchand and co-workers on the nature of the glass transition,[25,26] and the compositional dependence of the floppy to rigidity transition that occur in glass forming binary alloy systems including a-$Se_{1-x}Ge_x$.

The studies of Boolchand and co-workers[25,26] have established that: (i) there are two transitions are associated with the transition from *floppy* or underconstrained bonding in a-Se, to *rigid* or overconstrained bonding in an alloy with 33% Ge, or $GeSe_2$, and (ii) that these transitions span a *self-organized* compositional regime that is strain-free.[26] The first of these transitions occurs at the onset of average *local bonding rigidity* at a composition of $GeSe_4$. This composition corresponds to an average number of bonds/atom of 2.4, and an average number of bonding constraints/atom of 3, so that alloy compositions with increasing Ge content are overconstrained on average. However, the onset of *global bonding rigidity* is delayed by self-organization into nonstatistical bonding arrangements that minimize the total bond strain. These reorganizations occur up to a composition at which local bond strain percolates throughout the entire volume of the alloy. At this composition point global bonding rigidity sets in and the alloy is macroscopically overconstrained.[25,26]

Lucovsky, Phillips and co-workers in Refs. 21 and 22 pointed out that $Si–SiO_2$ interfaces were heterostructures in which the substrate Si could be considered as *rigid or overconstrained* with the N_{av} equaling exactly four, and the SiO_2 dielectric as ideal or *elastically compliant*. Since there is a transition region with a bonding chemistry intermediate between Si and SiO_2 that separates these two regions, comparisons with the a-$Se_{1-x}Ge_x$ chalcogenide alloy system can provide additional insights into the properties of the interfacial transition regions.

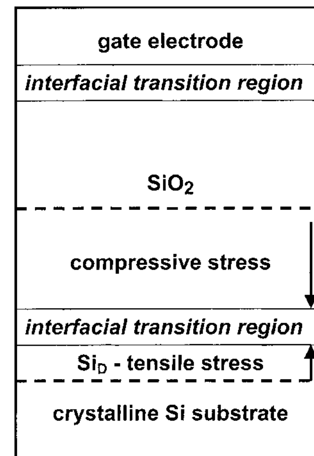

FIG. 5. Strain profile in an SiO_2 gate stack after a 900 °C anneal.

It has been demonstrated above that after a thermal anneal at 900 °C, there is: (i) a region of strained or defective Si in tensile stress in the Si substrate and (ii) a transition region with an average SiO composition that is approximately 1 molecular layer thick, ~0.3 nm. Building on the understanding of bond-strain driven self-organization in binary glass alloys such as Ge_xSe_{1-x},[25,26] this identifies an approach for describing the changes in bonding within the $Si–SiO_2$ interface transition region that occur after annealing at 900 °C. The interfacial transition region provides a continuous and smooth *transition* between intrinsic and thermally induced elastic tensile stress in the Si substrate and elastic compressive stress in the SiO_2 layer. Since this transition region *bridges* a rigid silicon substrate, and a *compliant or underconstrained* SiO_2 dielectric, the interfacial transition region plays the same role as the *strain-free compositional regime* in Ge_xSe_{1-x} alloys. Viewed in this way, the bonding changes after the 900 °C anneal are in effect a strain-driven self-organization that prevents the percolation of in-plane rigidity in the interfacial region, and thereby provides a strain-free region that bridges the Si substrate to the SiO_2 dielectric (see Fig. 5).

VII. ELECTRICAL PROPERTIES AND RELIABILITY CHANGES FROM INTERFACIAL SELF-ORGANIZATION

Figure 7 presents in a schematic representation the strain profile, defects, and defect precursors foran $Si–SiO_2$ heterostructure that includes a strain-free, self-organized interfacial transition region. Based that special properties with respect the absence of defect formation and/or changes in properties that chalcogenide alloy glasses and thin films display in the compositional regime between the onset of local bonding rigidity, and global or percolated bonding rigidity, the analogy in Fig. 6 assumes *similar special properties* for the in-

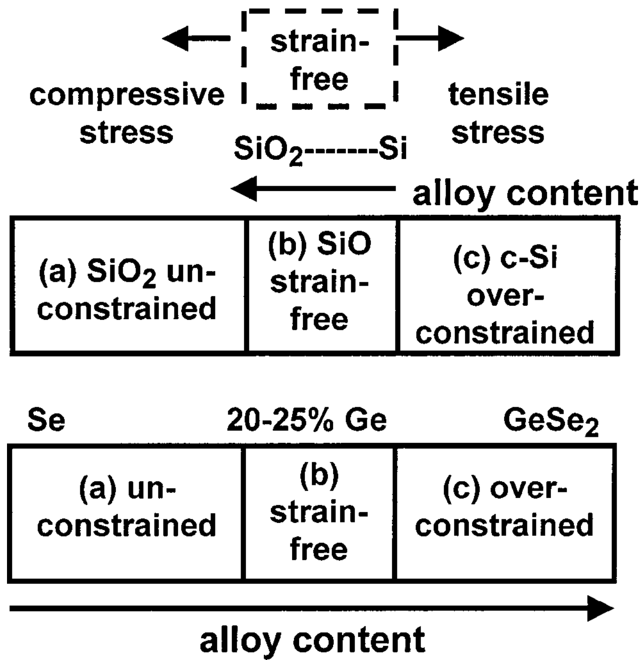

FIG. 6. Schematic representation of stress in floppy, self-organized, and rigid regions of an SiO_2-SiO_x-Si structure, and the corresponding regions of the noncrystalline Ge_xSe_{1-x} alloy system in the range from Se to $GeSe_2$ ($x = 0.333$).

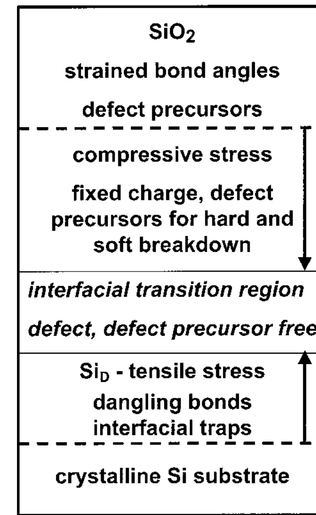

FIG. 7. Strain profile in an SiO_2 gate stack after a 900 °C anneal, including the regions in which defect and defect precursors are present.

terfacial transition region between the Si substrate and SiO_2 dielectric regions. The assumption of a strain free, self-organized interfacial transition region includes implicitly a scale for in-plane self-organization. Based on the density of dangling bonds in the tensile stressed Si substrate, this scale is estimated to be ~2.5 nm.

Channel mobilities have been extracted from the analysis of the current–voltage characteristics of FET devices using well-established techniques.[27] The mobility is plotted as a function of the electric field in the Si substrate normal to the plane of the interface. The mobilities are extracted from current–voltage plots based on an assumption that the density of charge carriers in the channel is determined by the capacitance of the SiO_2 dielectric film C_{ox} or equivalently from the value of EOT.[28] This leads to the *remarkable* result that electron and hole channel mobilities display universal dependencies that are determined by the same three physical properties of the interfacial region (i) the substrate doping that establishes the density of bulk charge defects within the channel region; (ii) a fixed charge Q_{int} within the SiO_2 dielectric that contributes to the scattering and determines the peak value of the mobility versus field; and (iii) an interface roughness parameter λ_{int} that defines the field dependence of the mobility in the high-field regime. The universality of electron and hole mobility curves derives from the empirical observation that to within an experimentally defined uncertainty, the values of Q_{int}, and an empirical roughness factor that includes a characteristic scattering length λ_{int} are the same. Q_{int} is approximately $2-5\times10^{10}\,cm^{-2}$, while λ_{int} is typically 2.5–3.0 nm. The value of λ_{int} is assumed in this article to represent the scale of self-organization within the interfacial transition region. The value of 2.5–3.0 nm is consistent with the assumption that the self-organization scale is the same as the *average distance* between Si substrate dangling bonds.

Consider next bonding defects. Prior to postmetallization annealing in a hydrogen-containing ambient such as forming gas, metal–oxide–semiconductor (MOS) devices with $Si-SiO_2$ interfaces display a defect density of dangling bonds that is in the low $10^{12}\,cm^{-2}$ regime.[17] These dangling bonds have been studied by electron spin resonance that reveals two interesting properties. First, the electron g factor displays the same symmetry of the Si substrate, and second, their number can be reduced by more than a factor of 50 by a postmetallization anneal (PMA) in a hydrogen-containing ambient. Third, these defects when not H terminated contribute to discrete interfacial defect features in the Si forbidden band gap that are revealed by capacitance–voltage ($C-V$) measurements. These results are consistent with these bonding defects being in the Si substrate, and in particular in the tensile stressed interfacial region designed in Fig. 7 as Si_D. The density of dangling bond defects prior to the PMAs, but after thermal annealing at 900 °C, is approximately constant and in the low $10^{12}\,cm^{-2}$ regime. It is independent of the way a device quality interface is formed, by thermal oxidation at a temperature in excess of 800 °C, or by an optimized remote plasma-assisted oxidation. These results are consistent with the precursor bonding arrangements for the interfacial self-organization being inherent in the empirically optimized thermal oxidation processes used throughout the semiconductor industry, and within other research groups preparing devices with optimized performance as well, in the optimized remote plasma assisted oxidation processes described in Refs. 29 and 30.

Figure 8 displays the density of interface traps D_{it} as a function of annealing temperature at a $Si(111)-SiO_2$ interface, prepared by thermal oxidation at 850 °C, furnace annealed at temperatures up to 1100 °C for 30 min in Ar, and

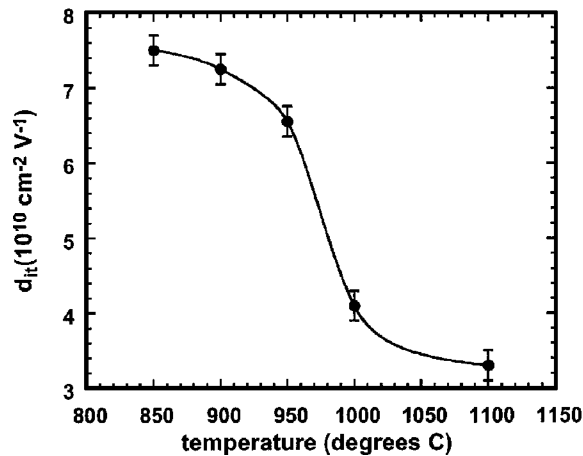

FIG. 8. Values of mid-gap densities of interface traps. d_{it}, extracted from $C-V$ measurements on Si(111) MOS structures as function of processing temperature. The solid line is an interpolation that establishes the trend in the data points.

then subjected to a PMA for 30 min at 400 °C in forming gas after the initial growth and following each annealing step.[4] Values of D_{it} have been determined from analysis of $C-V$ traces using standard techniques. The plot in Fig. 8 demonstrates that the most significant decreases in D_{it}, defined by numerical differentiation of the trace, occur at a temperature of ~975 °C, very close to the onset of the release of growth induced stress as in Ref. 12. In marked contrast, there is only a small decrease in D_{it} after the 900 °C anneal, indicating that these defects are not reduced significantly by the atomic rearrangements that occur during the interfacial transition region self-organization. This is consistent with these defects being resident in the Si substrate in the immediate vicinity of the interfacial transition region. This interpretation is also consistent with the universality of the energy dependence of D_{it} with respect to the Si valence and conduction band edges, and with the relatively narrow range of D_{it} reported for device-quality interfaces, independent of the processing using to create the interface. This is exemplified by the values of D_{it} for plasma processed and thermally grown interfaces, subjected to annealing at 900 and 1000 °C, and then to standard PMA procedures, forming gas anneals for at least 30 min at temperatures between 400 and 450 °C.

Experiments indicated that a direct correlation between D_{it} and the duration of remote plasma-assisted oxidation process used to form the Si–SiO_2 interface prior to SiO_2 deposition by remote plasma enhanced chemical vapor deposition.[29,30] The longer the process, the thicker the plasma oxidized film. This process is self-limiting in the sense that the thickness displays a power law dependence on time with a power law factor substantially smaller than one, ~0.2–0.25. In addition, the interface formation process determines the precursor arrangements for the interfacial layer that forms after the 900 °C anneal. The equivalence of a 300 °C plasma interface formation process that generates ~0.5–0.6 nm of oxide, and a thermal oxidation process at ~850–950 °C, with respect to interface self-organization has been established earlier in this article. As an example, the effect of longer plasma interface formation processes on the defect precursors that determine device reliability is presented in Figs. 9(a)–9(c).

Figures 9(a) and 9(b) presented plots of time dependent dielectric breakdown (TDDB) as a function of oxide bias for *p*MOS and *n*MOS FETs, respectively.[31] The traces marked 0.6 nm are for the optimized 300 °C plasma interface formation process, and the traces marked 0.8 nm are for a longer plasma process that increases D_{it}, and reduces channel current drive as well. The effect of the longer process time, and thicker interface layer prior to SiO_2 deposition and processing including high temperature anneals and PMAs is to reduce the TDDB time scale by a factor of 10, i.e., to reduce significantly device reliability. Figure 9(c) demonstrates a sixfold increase in stress induced leakage current after a 1000 s stress in a device with a 0.8 nm interfacial relative to an optimized device with a 0.6 nm interfacial oxide. These results suggest that interfaces formed by remote plasma oxidation at 300 °C create more extensive suboxide bonding arrangements, which are not optimally relaxed after the 900 °C anneal. This is of importance for device processing, and needs additional study.

Finally, the defects and defect precursors associated with nonoptimum interface formation, and strain in the Si substrate and SiO_2 layers, have been discussed in a general way with respect to Fig. 9. Based on the results discussed in this section of the article, it is concluded that: (i) Si atom dangling bonds and interface traps D_{it} are located in the strained Si substrate region designated as Si_D and (ii) the precursor states for soft and hard dielectric breakdown are in the strained SiO_2 film. Due to the relatively large Si–O–Si bond-angle distribution of $\sim\pm19°$ as displayed in Fig. 10,[32] there is a density of defect precursors in the portions of the SiO_2 that have minimal macroscopic intrinsic or thermally generated strain. These strained bonds contribute to defects and defect precursors as well, and it is not possible to make a persuasive argument for separating defects and/or defect precursors into two groups: one associated with macroscopic strain and a second associated with the Si–O–Si bond angle distribution. Si–O–Si bonds with bond angles between 130° and 150° are the least stable as based on their relative binding energy, and therefore are most easily further strained and by the macroscopic compress stress in the SiO_2 layers. These sites are candidates for the bond fission and breakdown. They are also the bonding sites that are chemically attacked by water,[33] and reduced in number in the formation of SiOF low-*k* films.[34]

VIII. SUMMARY

Studies of Si(111)–SiO_2 interfaces by optical second harmonic generation in Refs. 6–8 identified a strongly temperature dependent interfacial relaxation with an onset of ~900 °C. Coupled with determinations of D_{it} from $C-V$ measurements, the results presented in Ref. 6 differentiated between two distinctively different relaxations at Si–SiO_2 interfaces: one at approximately 850–900 °C associated with interface bonding changes, and a second at ~1000 °C asso-

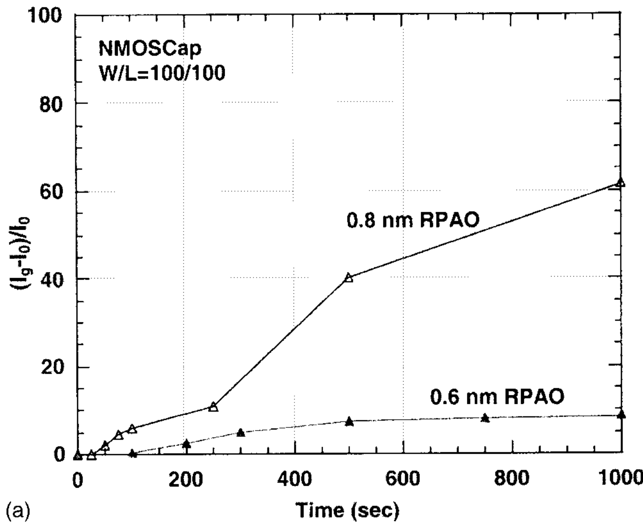

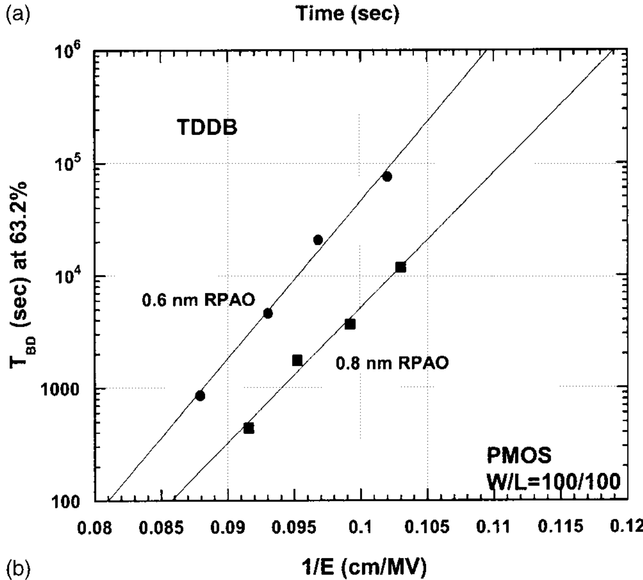

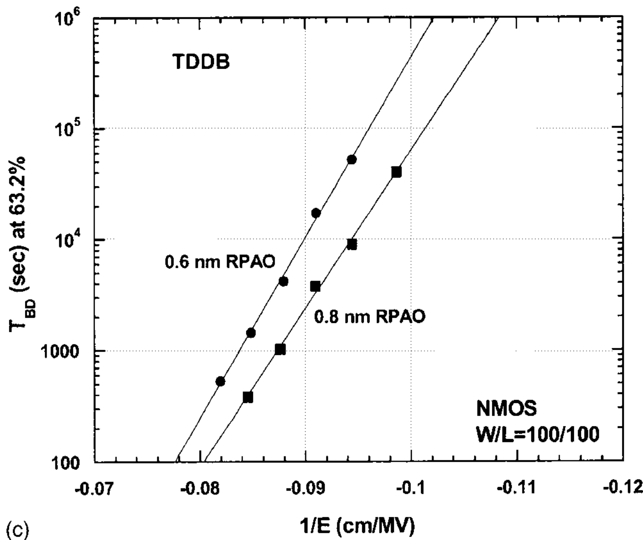

FIG. 9. (a) and (b) TDDB, a function of the reciprocal electrical stress field ($1/E$) for Si–SiO_x–Si oxynitride, $(SiO_2)_{0.5}(Si_3N_4)_{0.5}$, gate stacks for a different remote plasma assisted oxidation (RPAO) thickness of ~0.6 and ~0.8 nm. (c) Stress induced leak current for Si–SiO_x–Si oxynitride, $(SiO_2)_{0.5}(Si_3N_4)_{0.5}$, and gate stacks for a different RPAO thickness of ~0.6 and ~0.8 nm.

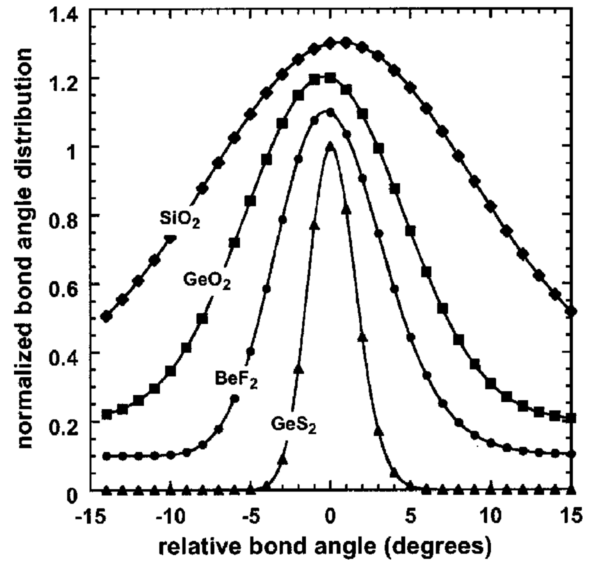

FIG. 10. Normalized bond angle distributions centered on the average bond angle at the two fold coordinated O-atom, F-atom, and S-atom bonding sites of SiO_2, GeO_2, BeF_2, and GeS_2 (Ref. 30).

ciated with relief of intrinsic compressive stress in the SiO_2 film. Complementary studies by SXPS have established that the interface relaxation is associated with changes in concentration and composition of suboxide bonding environments in an ultrathin interfacial transition region that is approximately 1 molecular layer thick (~0.3 nm). This relaxation occurs at a significantly lower temperature than the ~1000 °C relaxation of macroscopic compressive strain in the bulk of the SiO_2 film.[12] This article has provided important insights into these two distinct relaxation phenomena. It has demonstrated an analogy between: (i) the Si–SiO_2 interface in which there is a transition from a rigid substrate to an ideal random covalent network and (ii) compositionally dependent under- and overconstrained bonding in glass alloys such as Ge_xSe_{1-x}.[25,26] The interfacial suboxide transition region has been demonstrated to have properties in common with a regime of alloy compositions in which self-organization reduces bond constraint induced strain, thereby stabilizing these compositions against *aging*. This has provided important insights into defect formation at the semiconductor dielectric including Si–SiO_2 heterostructure in this article, as well as gate dielectric heterostructures that included deposited alternative dielectrics including Si oxynitride alloys (Si_3N_4) and alternative high-K dielectrics such as Al_2O_3 and transition metal and lanthanide rare earth oxides, and their respective silicate aluminate alloys. Metal silicate alloys have been discussed in Part II of this sequence of articles.

Finally, it is significant to note that several theoretical calculations have established that suboxide transition regions between c-Si and nc-SiO_2 are a natural consequence of the electronic structure.[35,36] In each of these calculations the extent of the suboxide region is at most a few molecular layers, consistent with the measurements and interpretation of the changes after self-organization reported in this article. There

have been many other studies of bonding at the Si–SiO_2 interface, including simulations of the thermal oxidation process. Some of the most recent ones are addressed in Ref. 37. It is hoped that the results presented in this article will stimulate computational physicists to address differences in the bonding between as-grown and annealed interfaces. Since dangling bond sites in the Si substrate have been proposed as nucleation sites for the self-organization, these computations can test that assumption as well.

ACKNOWLEDGMENTS

This research is in part supported by the Office of Naval Research (ONR), the semiconductor research corporation (SRC), and Microelectronics Advanced Research Corporation (MARCO). The authors wish to acknowledge helpful discussions with Professor Punit Boolchand of the University of Cincinnati.

[1]L. C. Feldman, L. Stensgard, P. J. Silverman, and T. E. Jackman, in *Proceedings of the International Conference on the Physics of SiO_2 and its Interfaces*, edited by S. T. Pantelides (Pergamon, New York, 1978), p. 344.
[2]D. E. Aspnes and J. B. Theeten, J. Electrochem. Soc. **127**, 1359 (1980).
[3]F. T. Himpsel, F. R. McFeely, J. A. Yarmoff, and G. Hollinger, Phys. Rev. B **38**, 6084 (1988).
[4]C. H. Bjorkman, T. Yasuda, C. E. Shearon, Jr., U. Emmerichs, C. Meyer, K. Leo, and H. Kurz, J. Vac. Sci. Technol. B **11**, 1521 (1993).
[5]J. Schafer, A. P. Young, L. J. Brillson, H. Niimi, and G. Lucovsky, Appl. Phys. Lett. **73**, 791 (1998).
[6]J. W. Keister, J. E. Rowe, J. J. Kolodziej, H. Niimi, H. S. Tao, T. E. Madey, and G. Lucovsky, J. Vac. Sci. Technol. A **17**, 1250 (1999).
[7]G. Wilk, R. W. Wallace, and J. M. Anthony, J. Appl. Phys. **89**, 5243 (2001), and references therein.
[8]International Technology Roadmap for Semiconductors ⟨http://public.itrs.net⟩ (2001).
[9]J. C. Phillips, J. Non-Cryst. Solids **34**, 153 (1979).
[10]J. C. Phillips, J. Non-Cryst. Solids **43**, 37 (1981).
[11]G. Lucovsky, H. Yang, H. Niimi, J. W. Keister, J. E. Rowe, M. F. Thorpe, and J. C. Phillips, J. Vac. Sci. Technol. B **18**, 1742 (2000).
[12]J. T. Fitch, C. H. Bjorkman, G. Lucovsky, F. H. Pollak, and X. Yim, J. Vac. Sci. Technol. B **7**, 775 (1988).
[13]G. Luepke, Surf. Sci. Rep. **35**, 75 (1999).
[14]C. H. Bjorkman, C. E. Shearon, Jr., Y. Ma, T. Yasuda, G. Lucovsky, U. Emmerichs, C. Meyer, K. Leo, and H. Kurz, J. Vac. Sci. Technol. A **11**, 964 (1993).
[15]U. Emmerichs *et al.*, J. Vac. Sci. Technol. B **12**, 2484 (1994).
[16]H. Yang, H. Niimi, J. W. Keister, and G. Lucovsky, IEEE Electron Device Lett. **21**, 76 (2000).
[17]R. Helms and E. H. Poindexter, Rep. Prog. Phys. **83**, 2449 (1998), and references therein.
[18]B. J. Hinds, F. Wang, D. M. Wolfe, C. L. Hinkle, and G. Lucovsky, J. Vac. Sci. Technol. B **16**, 2171 (1998).
[19]R. Carius, R. Fischer, E. Holzenkämpfer, and J. Stuke, J. Appl. Phys. **52**, 4241 (1981).
[20]*Binary Alloy Phase Diagrams*, 2nd ed. (ASM International, Materials Park, OH, 1990).
[21]J. C. Phillips, J. Vac. Sci. Technol. B **17**, 1803 (1999).
[22]G. Lucovsky, Y. Wu, H. Niimi, V. Misra, and J. C. Phillips, Appl. Phys. Lett. **74**, 2005 (1999).
[23]J. L. Whitten, Y. Zhang, M. Menon, and G. Lucovsky, J. Vac. Sci. Technol. B **20**, 1710 (2002).
[24]G. Lucovsky and J. C. Phillips, Appl. Phys. A: Mater. Sci. Process. **78**, 453 (2004).
[25]P. Boolchand, in *Insulating and Semiconducting Glasses*, edited by P. Boolchand (World Scientific, Singapore, 2000), p. 191.
[26]P. Boolchand, D. G. Georgiev, and M. Micoulaut, J. Optoelectron. Adv. Mater. **4**, 823 (2002).
[27]W. J. Zhu, J. P. Han, and T. P. Ma, IEEE Trans. Electron Devices **51**, 98 (2004).
[28]M. V. Fischetti, D. A. Neumayer, and E. A. Cartier, J. Appl. Phys. **90**, 4587 (2001).
[29]H. Niimi and G. Lucovsky, J. Vac. Sci. Technol. A **17**, 3185 (1999).
[30]H. Niimi and G. Lucovsky, J. Vac. Sci. Technol. B **17**, 2610 (1999).
[31]Y.-M. Lee, Ph.D. dissertation, North Carolina State University, 2003.
[32]G. Lucovsky, T. Morwer, L. S. Sremaniak, and J. L. Whitten, J. Non-Cryst. Solids **338–340**, 155 (2004).
[33]J. A. Theil, D. V. Tsu, S. S. Kim, and G. Lucovsky, J. Vac. Sci. Technol. A **8**, 1374 (1990).
[34]H. Yang and G. Lucovsky, J. Vac. Sci. Technol. A **16**, 1525 (1998).
[35]T. Tu and J. Tersoff, Phys. Rev. Lett. **84**, 4393 (2000).
[36]A. Bongiorno and A. Pasquarello, Appl. Phys. Lett. **83**, 1417 (2003)
[37]*Fundamental Aspects of Silicon Oxidation*, edited by Y. J. Chabal (Springer, Berlin, 2001).